

Dynamic Aspects in Host–Guest Interactions. 3. Kinetics and Mechanism for Molecular Recognition by Hexakis(2,6-di-*O*-methyl)- α -cyclodextrin of Some Azo Guest Molecules

Noboru Yoshida* and Yuji Fujita

Laboratory of Molecular Functional Chemistry, Division of Material Science, Graduate School of Environmental Earth Science, Hokkaido University, Sapporo 060, Japan

Received: October 4, 1994; In Final Form: December 12, 1994[⊗]

The inclusion reactions of some azo guest molecules, 3'-Pr-4'-(OH)Ph-N=N-PhSO₃⁻Na⁺ (**1**), 3'-iPr-4'-(OH)Ph-N=N-PhSO₃⁻Na⁺ (**2**), and 3'-tBu-4'-(OH)Ph-N=N-PhSO₃⁻Na⁺ (**3**), with hexakis(2,6-di-*O*-methyl)- α -cyclodextrin (DM- α CDx) were investigated. The rates and mechanism for the inclusion reactions of **1**, **2**, and **3** with DM- α CDx have been determined. Enhanced binding ability with the guest and a three-step inclusion mechanism by DM- α CDx were found.

Introduction

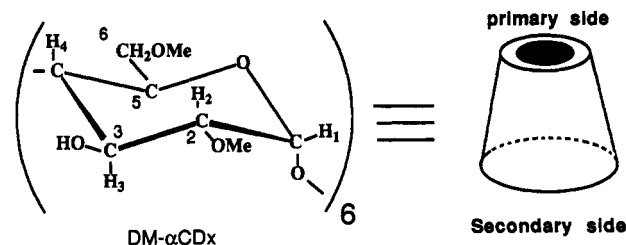
Kinetic studies of the inclusion reaction of cyclodextrins in aqueous solution, particularly by temperature-jump,¹ stopped-flow,² and time-resolved fluorescence³ techniques, have been an intense area of investigation. α -Cyclodextrin (α CDx) has received the most attention, largely because of its comprehensive clarification of the structural⁴ and mechanistic^{1,2} aspects of inclusion processes.

In general, the inclusion complexes in the solid state and in solution are mainly stabilized by van der Waals forces and, to a lesser extent, by dipole–dipole interactions.⁵ Hydrogen bonding seems to play a role in the formation of the inclusion complexes in apolar solvents and/or the crystalline state.⁶ In aqueous solution a further stabilization effect by hydrophobic interactions in which the solvent water pushes the hydrophobic site of the guest molecule into the hydrophobic CDx cavity has been observed. Therefore, methylation of the hydroxyl groups of α CDx would lead to the change in stability, solubility, and structure of the inclusion complexes.⁷ Hexakis(2,6-di-*O*-methyl)- α -cyclodextrin (DM- α CDx in Scheme 1) and hexakis(2,3,6-tri-*O*-methyl)- α -cyclodextrin (TM- α CDx) have been known as the methylated α CDx's. For example, the geometry of host–guest interactions such as TM- α CDx–benzaldehyde, *p*-iodophenol, and *p*-nitrophenol differs drastically from that of the corresponding native α CDx complexes because of the change in size and shape of the methylated α CDx as shown in Scheme 2.⁸

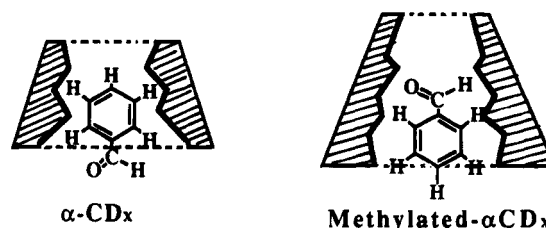
A series of the azo guest molecules was chosen for the present study because of the availability of comparable data from previous kinetic studies^{2c} in which the effects of the change in the size and shape of the substituents of the guests **1**, **2**, and **3** (Scheme 3) on the rate and mechanism for the inclusion reactions were investigated.

Recently, some progress has been made in understanding the mechanism of the inclusion reaction of α CDx.^{1,2} A two-step inclusion mechanism was found in the guest systems, **1**, **2**, and **3**.^{2c} The first step was ascribed to the fast association process with α CDx (k_{+1} and k_{-1}), and the subsequent slower process, to the intramolecular structural interconversion of the intermediate species (k_{+2} and k_{-2}) to attain a more stable final inclusion complex (Scheme 4).

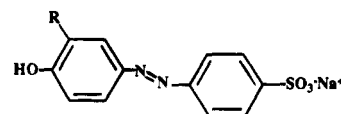
SCHEME 1



SCHEME 2



SCHEME 3



1: R = Pr, **2**: R = i-Pr, **3**: R = t-Bu

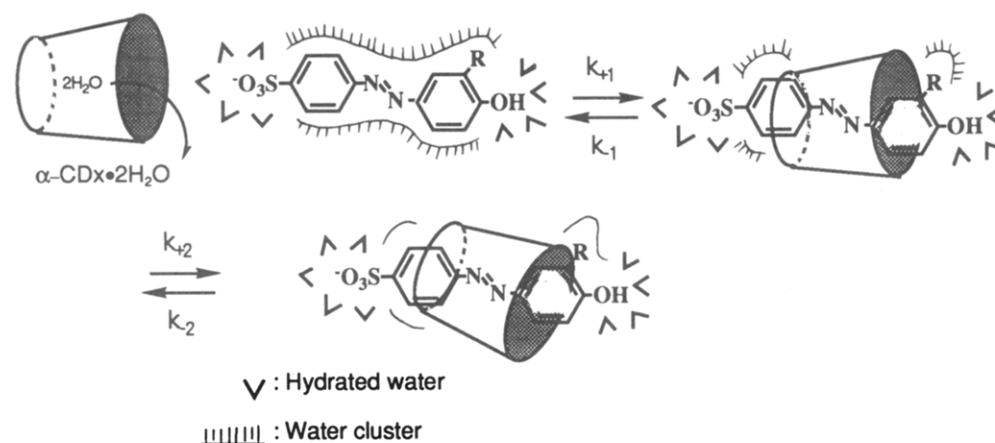
In this paper, the stability and kinetics of the interactions of azo guest molecules **1**, **2**, and **3** with DM- α CDx are described. The possible mechanistic aspects of the inclusion reactions in aqueous solution by DM- α CDx are also presented.

Experimental Section

Materials. Azo guest molecules were synthesized by the azo coupling method and purified by liquid column chromatography as described elsewhere.² α -Cyclodextrin was purchased from Tokyo Kasei Chemicals Co., Japan, and used without further purification. Hexakis(2,6-di-*O*-methyl)- α -cyclodextrin, heptakis(2,6-di-*O*-methyl)- β -cyclodextrin, and heptakis(2,3,6-tri-*O*-methyl)- β -cyclodextrin from Tohshin Chemicals Co., Japan, were used for most of the work reported here. Their melting point, $[\alpha]_D^{20}$, ¹H NMR spectral, and TLC data coincide well with those reported by Szejtli.⁹

[⊗] Abstract published in *Advance ACS Abstracts*, February 15, 1995.

SCHEME 4

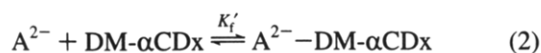


Measurements. Stability constants of the inclusion complexes were determined spectrophotometrically using a JASCO Ubest-30 spectrometer as previously described.² The kinetic measurements were performed using a Unisoku optical-fiber-type stopped-flow apparatus and a data acquisition system. Pseudo-first-order conditions of excess host concentrations ($[\text{DM-}\alpha\text{CDx}] = (0.4\text{--}4) \times 10^{-3} \text{ mol dm}^{-3}$) were maintained over the guest concentrations ($[\text{guest}] = (2\text{--}5) \times 10^{-5} \text{ mol dm}^{-3}$). Plots of $\ln(A_t - A_\infty)$ vs time gave a straight line for at least 3 half-lives. The observed pseudo-first-order rate constants (k_{obsd}) were determined from the average of three replicate measurements. The reaction temperature was maintained to within ± 0.1 °C at 25 °C by means of an external circulating water bath (Lauda Type K2R thermostat). The pH of the solution in the acidic and alkaline regions was maintained using phosphate buffer (pH 4.0–4.5) and NaOH (pH 11.0–11.5), respectively. The ionic strength was maintained at 0.1 mol dm^{-3} with NaCl.

Results and Discussion

2,6-Di-O-methylation Effect on Stability Constants. We have determined the stability constants for the inclusion complexes of the azo guest molecules **1**, **2**, and **3** with DM- αCDx using UV–visible spectrophotometric titrations at 25 °C and $I = 0.1 \text{ mol dm}^{-3}$ (NaCl). These azo guest molecules exist as the acid form (HA^-) in phosphate buffer solutions at pH 4.0–4.2 and the base form (A^{2-}) in NaOH solutions at pH 11–11.5, where H denotes the phenol proton (PhOH). Figure 1 shows the changes in the absorption spectra which occur when $3(\text{A}^{2-})$ binds to DM- αCDx .

Upon consecutive additions of excess DM- αCDx , the red shift (bathochromic effect) and decrease in intensity (hypochromic effect) of $\lambda_{\text{max}}(3(\text{A}^{2-}))$ in the visible region were induced. In the UV region, the red shift and the increase in intensity (hyperchromic effect) of $\lambda_{\text{max}}(3(\text{A}^{2-}))$ were observed. These spectral tendencies observed for the base form (A^{2-}) are the same as those of the acid form (HA^-) of **3**. Only the 1:1 inclusion model fits the titration data. Figure 2 shows the differential absorption spectra in the $3(\text{A}^{2-})\text{--DM-}\alpha\text{CDx}$ system. The clear existence of several isosbestic points may be related to the following simple 1:1 inclusion equilibria.



The stability constants K_f and K'_f presented in Table 1 were obtained by the Hildebrand–Benesi plot. The four to five

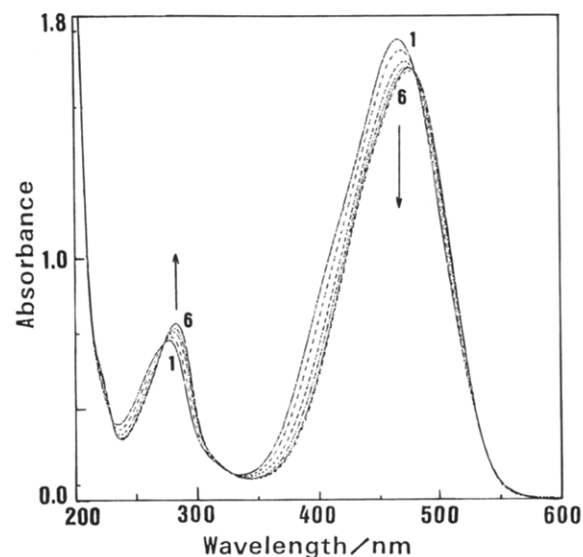


Figure 1. Spectral change of the base form (A^{2-}) of **3** at various DM- αCDx concentrations at 25 °C and $I = 0.1 \text{ mol dm}^{-3}$ (NaCl): (1) 0; (2) 6.72×10^{-5} ; (3) 2.24×10^{-4} ; (4) 4.48×10^{-4} ; (5) 1.34×10^{-3} ; (6) $2.24 \times 10^{-3} \text{ mol dm}^{-3}$. $[\text{3}] = 6.0 \times 10^{-5} \text{ mol dm}^{-3}$. pH = 11.5 (phosphate buffer).

different wavelengths at which the absorbance change in Figure 2 is larger are used, although similar but less accurate calculated stability constants are derived from other wavelengths. The data in Table 1 provide a comparison of the stability for the binding of **1**, **2**, and **3** with DM- αCDx under a variety of conditions, including variation of the size and shape of the phenol moiety ($3'\text{-R-}4'\text{-(OH)Ph-}$) of the guests, of the size and degree of methylation of the αCDx , and of pH. The stability constants K_f for the inclusion complexes of the acid form (HA^-) of **1**, **2**, and **3** with DM- αCDx are appreciably larger (ca. 4–7 times) than those for complexes with αCDx . On the other hand, *O*-methylation of the O(2)H and O(6)H hydroxyl groups of αCDx has less effect on the stability constants for the base forms (A^{2-}) of **1** and **2**. However, in the base form (A^{2-}) of the bulky guest molecule **3**, the value of K'_f for the DM- αCDx complex is ca. 5.5 times larger than that for the αCDx complex. Deprotonation of the hydroxyl group of the phenol moiety ($3'\text{-R-}4'\text{-(OH)Ph-}$) of the guest **3** has little effect on the stability of the DM- αCDx inclusion complex ($K_f \sim K'_f$). The alkyl substituents Pr, *i*Pr, and *t*Bu on the phenol side of **1**, **2**, and **3** affect appreciably the stabilities of the $\text{HA}^- \text{--DM-}\alpha\text{CDx}$ inclusion complexes. The stability constants for the HA^- species were found to decrease in the order $1 > 2 > 3$, as was already pointed out for the αCDx system.^{2d}

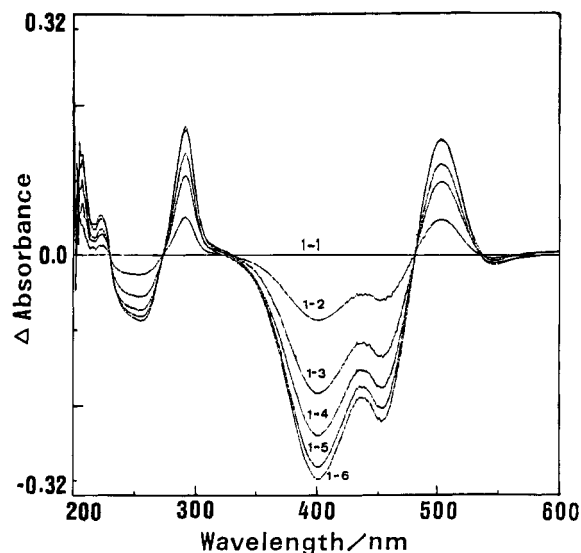


Figure 2. Differential absorption spectra between spectrum 1 and spectra 2–6 in Figure 1. Some clear isosbestic points are observed in the wider range of the concentration change of DM- α CDx.

TABLE 1: Binding Constants K_f (M^{-1})^a and K_f' (M^{-1}) for Complexation of α CDx and DM- α CDx with the Azo Guests 1, 2, and 3^b

guest molecule	pK_a	α CDx		DM- α CDx	
		K_f^c	$K_f'^d$	K_f	K_f'
1	8.19 ^e	8300 ^e	7100 ^e	49000 (± 5000)	11000 (± 3000)
		7500 (± 300)	6900 (± 150)		
2	8.12 ^e	4500 ^e	5000 ^e	27000 (± 2000)	12000 (± 2000)
		3100 (± 200)			
3	8.70 ^e	1900 ^e	1100 ^e	7400 (± 900)	6000 (± 300)

^a $M = \text{mol dm}^{-3}$. ^b At 25 °C and $I = 0.1 \text{ mol dm}^{-3}$ (NaCl). ^c $K_f = [\text{HA}^- - \text{CDx}]/([\text{HA}^-][\text{CDx}])$. ^d $K_f' = [\text{A}^{2-} - \text{CDx}]/([\text{A}^{2-}][\text{CDx}])$. ^e Reference 2d.

TABLE 2: Binding Constants K_f (M^{-1}) and K_f' (M^{-1}) for Complexation of β CDx, DM- β CDx, and TM- β CDx with the Azo Guests 1, 2, and 3^a

guest molecule	β CDx		DM- β CDx		TM- β CDx	
	K_f	K_f'	K_f	K_f'	K_f	K_f'
1	5600 ^b	2900 ^b	20000 (± 4000)	6400 (± 200)	5500 (± 900)	3100 (± 100)
	3300 (± 50)	1800 (± 100)				
2	2500 ^b	1700 ^b	22000 (± 2000)	7100 (± 400)	3600 (± 200)	1600 (± 200)
3	3400 ^b	1700 ^b	22000 (± 2000)	4400 (± 500)	4700 (± 1500)	1300 (± 200)

^a At 25 °C and $I = 0.1 \text{ mol dm}^{-3}$ (NaCl). ^b Reference 2d.

Further investigation of the methylation effect on the stability of the inclusion complexes was carried out for the DM- β CDx and TM- β CDx systems. As shown in Table 2, the stability constants for the DM- β CDx inclusion complexes of HA⁻ (1, 2, and 3) are ca. 6–9 times larger than those for β CDx inclusion complexes. As is different from the DM- α CDx system, this enhanced stability was observed (ca. 4 times) also in the A²⁻ (1, 2, and 3)-DM- β CDx system. It should be noted that the substitution by a methyl group at the O(2) or O(6) position in β CDx lengthens the cavity from ca. 8 to 11 Å and enhances the inclusion ability.¹⁰ An X-ray diffraction study by Harata¹¹ also suggested the fact that the methylation of the O(2)H and

O(6)H hydroxyl groups of β CDx makes the cavity deeper without any significant distortion of the macrocyclic ring because the O(3)H hydroxyl groups can retain the intramolecular hydrogen bond O(3)H...O(2) (see Scheme 1).

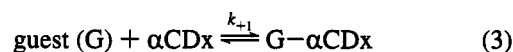
In general, the DM- β CDx inclusion complex of the A²⁻ species of 1, 2, and 3 is appreciably less stable than those of the corresponding HA⁻ species, which was already pointed out in the β CDx system. The decreased values of the stability constant ($K_f' < K_f$) reflect the increasing hydrophilicity of the phenol moiety of the guests due to the ionization of the hydroxyl group (3'-R-4'-(OH)Ph- \rightarrow 3'-R-4'-(O⁻)Ph-).

Thus, 2,6-di-*O*-methylation of α - and β -cyclodextrin increases the stability of their inclusion complexes of both HA⁻ and A²⁻ species of 1, 2, and 3 in aqueous solution, possibly because the methyl groups at the O(2) position of DM- α CDx and DM- β CDx provide a more hydrophobic environment around the host cavity, thereby favoring effective hydrophobic interactions that stabilize the complexes. In addition, further stabilization could also be obtained by capping of one side of the macrocycle by the methylation of the primary O(6)H hydroxyl groups, which significantly improves the binding ability with the guests.¹² These stabilization effects found in the DM- β CDx system have been observed in other guest system such as *p*-nitrophenol.¹³ An enhanced transport rate in the liquid membrane of neutral azobenzene derivatives by DM- β CDx has also been reported.¹⁴ On the other hand, very little effect on the binding constants with DM- β CDx for sodium *m*- and *p*-nitrophenolates has been pointed out by Armstrong et al. using a high-dilution calorimetric technique.¹⁵

Further methylation as observed in 2,3,6-tri-*O*-methylated β CDx (TM- β CDx) would reduce considerably the stability of their inclusion complexes. As summarized in Table 2, the stability of the TM- β CDx complexes decreases appreciably as compared with that of the corresponding DM- β CDx complexes. Perhaps, further substitution by *O*-methyl groups at the inner side (the O(3)H group) of β CDx narrows the inner diameter of the cavity. An X-ray diffraction study demonstrates that, in contrast to the case of DM- β CDx, the macrocyclic ring is distorted in the fully-methylated cyclodextrin and the steric hindrance involving methyl groups enlarges the O(2), O(3) end of cavity.¹¹

Our equilibrium studies about the nature of the *O*-methylation effect of α - and β CDx upon the stability of various inclusion complexes suggest the importance of the position and number of *O*-methyl groups on the rim of CDx molecules.

2,6-Di-*O*-methylation Effect on the Kinetics and Mechanism. In most inclusion reactions with α CDx, one relaxation signal has been generally observed.^{1a-c} Therefore, the observed rate constant (k_{obsd}) increases linearly with the total concentration of α CDx ($[\alpha\text{CDx}]_T$) and its concentration dependence is simply interpreted by the following one-step reaction mechanism.



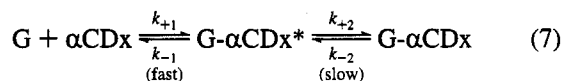
$$k_{\text{obsd}} = k_{+1}[\alpha\text{CDx}]_T + k_{-1} \quad (4)$$

In recent work,^{2c,e} it was discovered that some azo guest molecules were included in the α CDx cavity through the two-step mechanism (Scheme 4). Two relaxation signals have been clearly observed in the fast (millisecond) and slow (second) time regions. The dependence of $k_{\text{obsd}}(\text{fast})$ vs $[\alpha\text{CDx}]_T$ is linear, but that of $k_{\text{obsd}}(\text{slow})$ approaches a saturated value against the higher $[\alpha\text{CDx}]_T$. Thus, the following rate expressions were demonstrated:

$$k_{\text{obsd}}(\text{fast}) = k_{+1}[\alpha\text{CDx}]_{\text{T}} + k_{-1} \quad (5)$$

$$k_{\text{obsd}}(\text{slow}) = \frac{K_1 k_{+2} [\alpha\text{CDx}]_{\text{T}}}{(1 + K_1 [\alpha\text{CDx}]_{\text{T}})} + k_{-2} \quad (6)$$

where K_1 is equal to the ratio k_{+1}/k_{-1} . These host-concentration dependencies of k_{obsd} could be interpreted generally in terms of the following two-step inclusion mechanism, where the first step



is a fast binding process of the guest (G) with αCDx and the second step is a subsequent slower intramolecular structural interconversion of the intermediate species ($\text{G}-\alpha\text{CDx}^*$), which is in slower equilibrium with a more stable final inclusion complex ($\text{G}-\alpha\text{CDx}$). If the first step is immeasurably fast by the relaxation technique such as the stopped-flow method, only the slow step is observed and the rate expression of eq 6 is valid.^{1d,f}

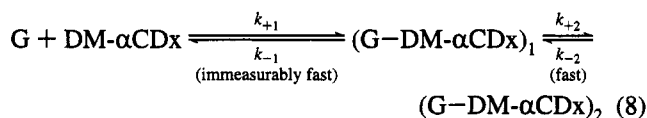
For the guest **1**, both the fast step and the slow step in the inclusion with αCDx could be independently monitored.^{2c,e} The rate constants k_{+1} , k_{-1} , k_{+2} , and k_{-2} for the HA^- species were $2.0 \times 10^4 \text{ mol}^{-1} \text{ dm}^3 \text{ s}^{-1}$, 6.0 s^{-1} , 0.87 s^{-1} , and 0.55 s^{-1} , respectively (Scheme 4). The rate constants for the A^{2-} species were almost the same as those for the HA^- species and were determined to be $6.9 \times 10^3 \text{ mol}^{-1} \text{ dm}^3 \text{ s}^{-1}$, 3.6 s^{-1} , 0.25 s^{-1} , and 0.08 s^{-1} , respectively. The guest **2** also shows similar kinetic behavior. The rate constants k_{+1} , k_{-1} , k_{+2} , and k_{-2} for the $\text{HA}^-(\mathbf{2})$ species were $1.2 \times 10^4 \text{ mol}^{-1} \text{ dm}^3 \text{ s}^{-1}$, 9.4 s^{-1} , 0.58 s^{-1} , and 0.26 s^{-1} , respectively. However, in the case of guest **3**, the reaction is considerably slower in the range of seconds and proceeds as a one-step mechanism which would contain only the binding step with αCDx . The reduced rate constants (k_{+1} and k_{-1}) for the $\text{HA}^-(\mathbf{3})$ species have been obtained as $4.6 \times 10^2 \text{ mol}^{-1} \text{ dm}^3 \text{ s}^{-1}$ and 0.55 s^{-1} , respectively. This is interpreted as a result of an increase of steric repulsion in the transition state between the rim of αCDx and the bulky *t*Bu group of **3**.

Contrary to our anticipation, the kinetics of the inclusion reaction with $\text{DM}-\alpha\text{CDx}$ is more complicated than that with αCDx as mentioned above. The kinetic inclusion behavior of $\text{DM}-\alpha\text{CDx}$ is more surprising than its unusual inclusion stability with the guests. Figure 3 represents an interesting comparison of the stopped-flow signals at $340(\lambda_{\text{HA}^-})$ and $390(\lambda_{\text{A}^{2-}})$ nm for the inclusion reactions of **3** with αCDx and $\text{DM}-\alpha\text{CDx}$, respectively.

The two relaxation curves for both $\mathbf{3}(\text{HA}^-)$ and $\mathbf{3}(\text{A}^{2-})$ in the presence of $\text{DM}-\alpha\text{CDx}$ exhibit some interesting differences if compared to those for the $\alpha\text{CDx}-\mathbf{3}(\text{HA}^-)$ and $-\mathbf{3}(\text{A}^{2-})$ systems. An unusual rapid process which is not observed in the αCDx system (vide infra) is found in the $\text{DM}-\alpha\text{CDx}$ system prior to the usual time region. The contribution of the rapid process to the overall change is somewhat different in the acid (HA^-) and base (A^{2-}) forms of **3** (parts C and D) in Figure 3). The pseudo-first-order rate constants $k_{\text{obsd}}(\text{fast})$ of this fast step are plotted against $[\text{DM}-\alpha\text{CDx}]_{\text{T}}$ in the inclusion reaction of $\mathbf{3}(\text{HA}^-(\text{O}))$ and $\mathbf{3}(\text{A}^{2-}(\Delta))$ in Figure 4.

Since the two plots almost overlap, the step in $\mathbf{3}(\text{HA}^-(\text{O}))$ would be the same process as observed in $\mathbf{3}(\text{A}^{2-}(\Delta))$ and possibly also in $\mathbf{2}(\text{HA}^-(\square))$. Interestingly, these plots are clearly not linear, showing that prior to the monitored fast process there would be a more rapid equilibrium between the guest and the host. Therefore, it is suggested that the mechanism which

includes two inclusion species, $(\text{G}-\text{DM}-\alpha\text{CDx})_1$ and $(\text{G}-\text{DM}-\alpha\text{CDx})_2$, is conceivable for this monitored fast step. Thus, the following inclusion mechanism is presented as the fast relaxation process.



Since the association process between $\text{DM}-\alpha\text{CDx}$ and **3** is not monitored by our stopped-flow method, the following relation and rate expression is obtained under the condition of $[\text{DM}-\alpha\text{CDx}]_{\text{T}} > (\mathbf{3})_{\text{T}}$.^{2c,e}

$$k_{+1}[\text{DM}-\alpha\text{CDx}]_{\text{T}} + k_{-1} \gg k_{+2} + k_{-2} \quad (9)$$

$$k_{\text{obsd}}(\text{fast}) = \frac{K_1 k_{+2} [\text{DM}-\alpha\text{CDx}]_{\text{T}}}{(1 + K_1 [\text{DM}-\alpha\text{CDx}]_{\text{T}})} + k_{-2} \quad (10)$$

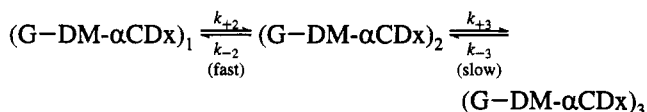
In equation 10, $K_1 = k_{+1}/k_{-1} = [(\text{G}-\text{DM}-\alpha\text{CDx})_1]/[\text{G}][\text{DM}-\alpha\text{CDx}]$ is the equilibrium constant for the association step between host and guest. At high $[\text{DM}-\alpha\text{CDx}]_{\text{T}}$, $K_1[\text{DM}-\alpha\text{CDx}]_{\text{T}} > 1$ and $k_{\text{obsd}}(\text{fast}) = k_{+2} + k_{-2}$ (the saturated value in Figure 4). At low $[\text{DM}-\alpha\text{CDx}]_{\text{T}}$, $K_1[\text{DM}-\alpha\text{CDx}]_{\text{T}} \ll 1$ and $k_{\text{obsd}}(\text{fast}) = K_1 k_{+2} [\text{DM}-\alpha\text{CDx}]_{\text{T}} + k_{-2}$ (the linear dependence in Figure 4). Equation 10 was rearranged into eq 11.

$$(k_{\text{obsd}}(\text{fast}) - k_{-2})^{-1} = (K_1 k_{+2} [\text{DM}-\alpha\text{CDx}]_{\text{T}})^{-1} + (k_{+2})^{-1} \quad (11)$$

A good estimation of k_{-2} leads to a linear plot of $(k_{\text{obsd}}(\text{fast}) - k_{-2})^{-1}$ vs $([\text{DM}-\alpha\text{CDx}]_{\text{T}})^{-1}$, and the values of $(K_1 k_{+2})^{-1}$ and $(k_{+2})^{-1}$ are determined from the slope and the intercept, respectively, as shown in Figure 5.

The values of k_{+2} , k_{-2} and K_1 were estimated with a trial and error process. The estimated rate constants and equilibrium constants for the fast step are summarized in Table 3.

Furthermore, in the $\mathbf{3}-\text{DM}-\alpha\text{CDx}$ system, the slow step is observed as already shown in Figure 3. Also in the slow step, the saturated-type dependence of the rate constant is clearly observed (Figure 6). This saturated type concentration dependency of $k_{\text{obsd}}(\text{slow})$ for the slow step could be simply interpreted as the following reorganization process of the intermediate species $(\text{G}-\text{DM}-\alpha\text{CDx})_2$ into the final inclusion complex $(\text{G}-\text{DM}-\alpha\text{CDx})_3$.



In most cases, the plots of $(k_{\text{obsd}}(\text{slow}) - k_{-3})^{-1}$ vs $[\text{DM}-\alpha\text{CDx}]_{\text{T}}^{-1}$ are linear and thus $(K_2 k_3)^{-1}$ and $(k_3)^{-1}$ are estimated from the slope and the intercept of the plot, respectively. In some cases, a small concentration dependence of $k_{\text{obsd}}(\text{slow})$ is observed. This is interpreted as being because, since $K_2[\text{DM}-\alpha\text{CDx}]_{\text{T}} \gg 1$, $k_{\text{obsd}}(\text{slow})$ closely approaches $k_{+3} + k_{-3}$. This is the case for the $\mathbf{1}(\text{A}^{2-})$ and $\mathbf{2}(\text{HA}^-)$ systems. The obtained rate constants, k_{+3} and k_{-3} , and/or the sum of the rate constants, $k_{+3} + k_{-3}$, for the third step are given in Table 3.

The kinetic result obtained for the $\mathbf{1}-\text{DM}-\alpha\text{CDx}$ system is somewhat different from those described above. Figure 7 represents a plot of $k_{\text{obsd}}(\text{fast})$ for $\mathbf{1}(\text{HA}^-)$ and $\mathbf{1}(\text{A}^{2-})$ as a function of $\text{DM}-\alpha\text{CDx}$ concentration. The plot for $\mathbf{1}(\text{HA}^-)$ becomes more curved than that for $\mathbf{1}(\text{A}^{2-})$ with increasing

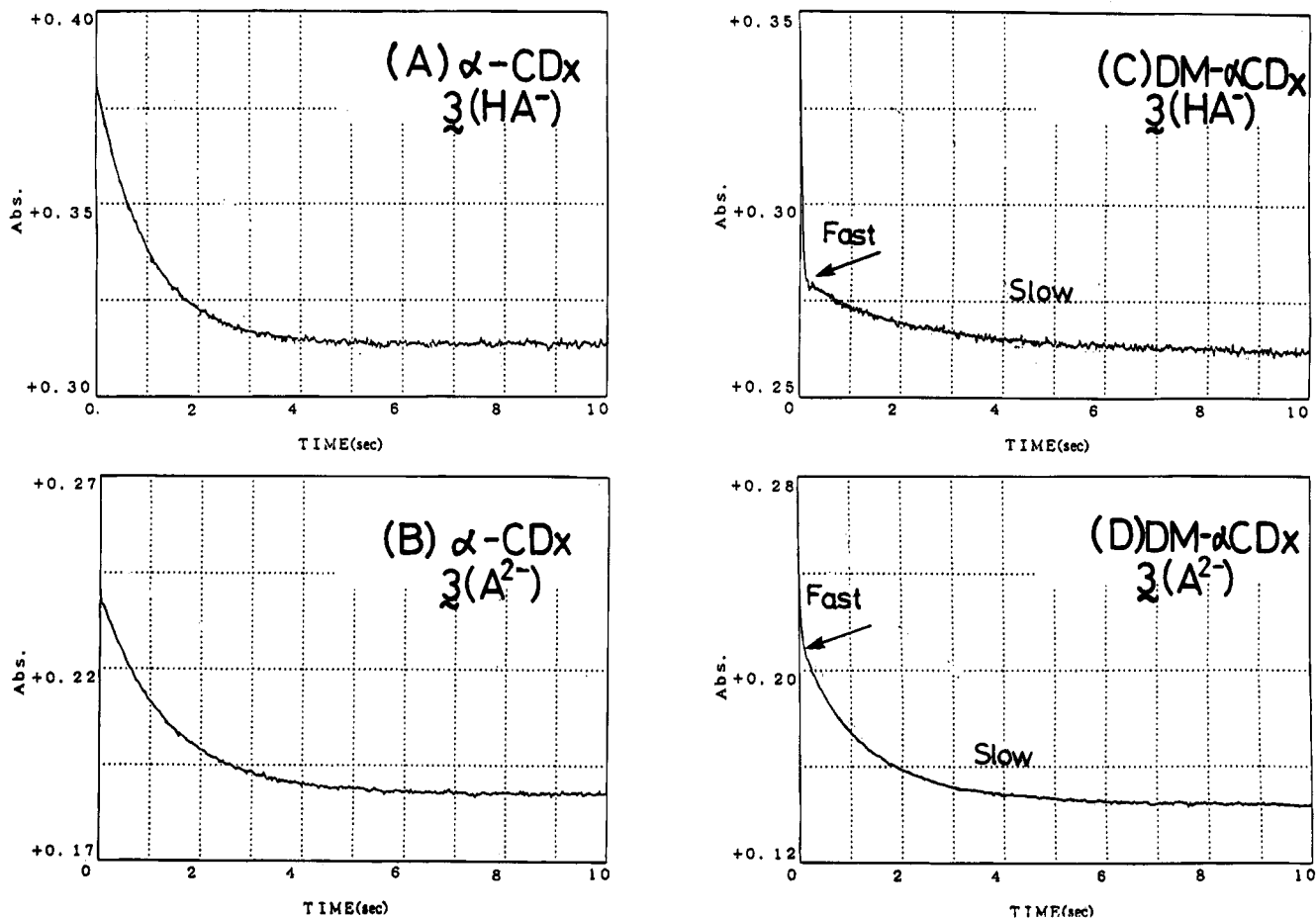


Figure 3. Comparison of the stopped-flow signals for the change in absorbance of the binding process of $3(\text{HA}^-)$ and $3(\text{A}^{2-})$ with α -cyclodextrin and DM- α -cyclodextrin. In the binding process with DM- α -CDx, both the fast step and the slow step are observed. The arrow denotes the break point between the fast and the slow process. (A) $[3(\text{HA}^-)] = 3.0 \times 10^{-5} \text{ mol dm}^{-3}$ and $[\alpha\text{CDx}] = 1.2 \times 10^{-3} \text{ mol dm}^{-3}$ at $\lambda_{\text{obs}} = 340 \text{ nm}$ and $\text{pH} = 4.6$; (B) $[3(\text{A}^{2-})] = 3.0 \times 10^{-5} \text{ mol dm}^{-3}$ and $[\alpha\text{CDx}] = 1.2 \times 10^{-3} \text{ mol dm}^{-3}$ at $\lambda_{\text{obs}} = 390 \text{ nm}$ and $\text{pH} = 11.5$; (C) $[3(\text{HA}^-)] = 3.0 \times 10^{-5} \text{ mol dm}^{-3}$ and $[\text{DM-}\alpha\text{CDx}] = 1.2 \times 10^{-3} \text{ mol dm}^{-3}$ at $\lambda_{\text{obs}} = 340 \text{ nm}$ and $\text{pH} = 4.6$; (D) $[3(\text{A}^{2-})] = 3.0 \times 10^{-5} \text{ mol dm}^{-3}$ and $[\text{DM-}\alpha\text{CDx}] = 1.2 \times 10^{-3} \text{ mol dm}^{-3}$ at $\lambda_{\text{obs}} = 390 \text{ nm}$ and $\text{pH} = 11.5$.

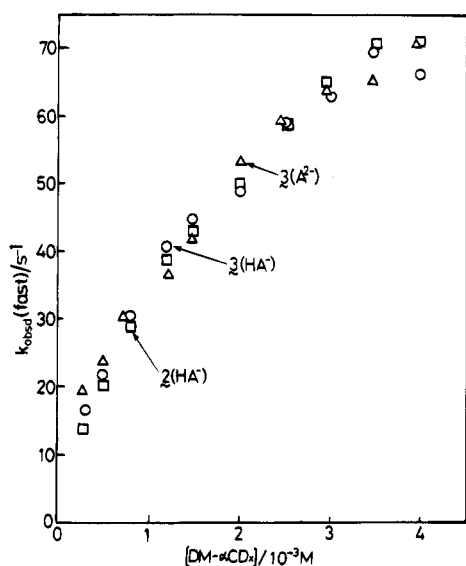


Figure 4. Plots of the observed rate constants $k_{\text{obsd}}(\text{fast})$ vs $[\text{DM-}\alpha\text{CDx}]$ for the fast step of the inclusion reactions of $3(\text{HA}^-)$ (○), $3(\text{A}^{2-})$ (△), and $2(\text{HA}^-)$ (□) with DM- α CDx.

concentration of DM- α CDx. Additionally, the slow inclusion step may not be observed in the acid form (HA^-) of 1. This might be explained through the directional binding from the alkyl phenol moiety of $1(\text{HA}^-)$ for which steric hindrance is

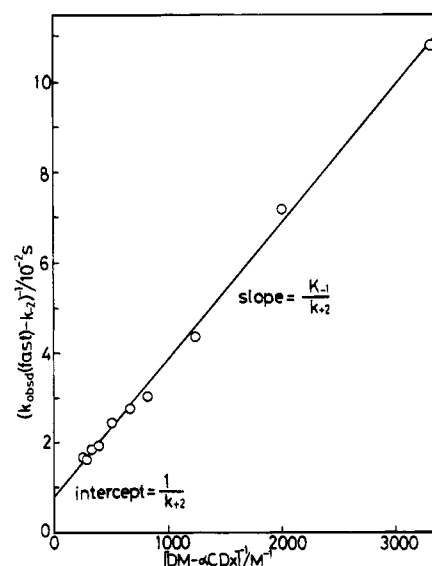


Figure 5. Plot of $(k_{\text{obsd}}(\text{fast}) - k_{-2})^{-1}$ vs $[\text{DM-}\alpha\text{CDx}]^{-1}$ for the fast step of the inclusion reaction of $3(\text{HA}^-)$ with DM- α CDx and the calculated line using data from the least-squares fit: $k_{-2} = 6 \text{ s}^{-1}$, $K_1 = 264 \text{ M}^{-1}$, and $k_{+2} = 130 \text{ s}^{-1}$.

smaller. In this case, a larger K_1 value for the association step is anticipated. The Corey-Pauling-Koltun molecular model indicates that the inclusion of the alkyl phenol moiety of guest

TABLE 3: Rate^a and Equilibrium Constants for the Inclusion Reactions of DM- α -Cyclodextrin with the Guest Molecules, 1–3, at 25 °C and $I = 0.1 \text{ mol dm}^{-3}$ (NaCl)

guest molecule	HA ⁻ species					A ²⁻ species				
	K_1/M^{-1}	k_{+2}/s^{-1}	k_{-2}/s^{-1}	k_{+3}/s^{-1}	k_{-3}/s^{-1}	K_1'/M^{-1}	k_{+2}'/s^{-1}	k_{-2}'/s^{-1}	k_{+3}'/s^{-1}	k_{-3}'/s^{-1}
1	$\sim 480^b$	$\sim 60^b$	$\sim 7.0^b$	<i>c</i>	<i>c</i>	120	200	0.5	0.1–0.2	
2	270	140	3.0	~ 0.2		65	330	5.0	~ 4.0	$(k_{+3}' + k_{-3}')^d$
3	260^e	130^e	6.0^e	~ 0.7	~ 0.3	$\sim 200^d$	$\sim 120^d$	$\sim 10^d$	$\sim 5.0^e$	$\sim 0.4^e$

^a Error limits are estimated to be not larger than $\pm 10\%$ and $\pm 20\%$ in any determination of $k_{+2}(k_{+2}')$ and $k_{-2}(k_{-2}')$, respectively, unless otherwise noted. ^b The equilibrium and the rate constants are estimated with a large experimental error ($> \pm 50\%$). ^c Not detected in the slower time region. ^d The change of absorbance accompanying the reaction is too small to determine the exact value. ^e Main reaction. The contribution of the absorption change of the other reaction to the overall change is considerably small, as shown in Figure 3.

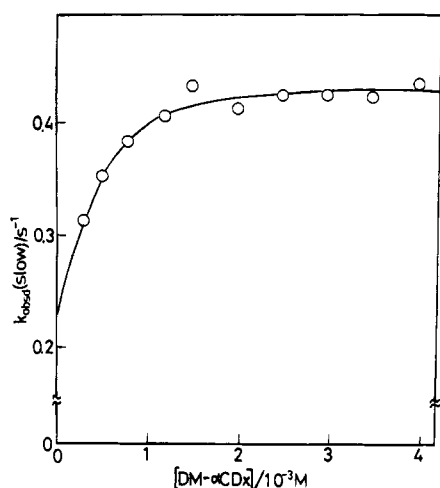


Figure 6. Plot of the observed rate constants $k_{\text{obsd}}(\text{slow})$ vs $[\text{DM-}\alpha\text{CDx}]$ for the slow step of the inclusion reactions of **2**(A²⁻) and DM- α CDx. The calculated curve was drawn using the data from the least-squares fit: $k_3 = 0.4 \text{ s}^{-1}$ and $k_{-3} = 0.2 \text{ s}^{-1}$.

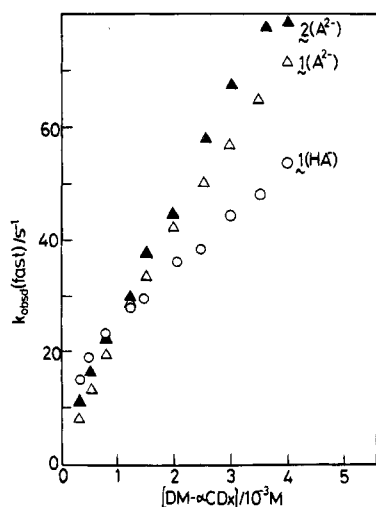
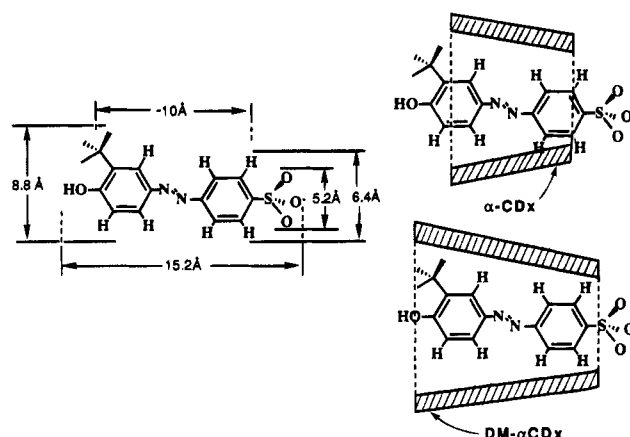


Figure 7. Plots of the observed rate constants $k_{\text{obsd}}(\text{fast})$ vs $[\text{DM-}\alpha\text{CDx}]$ for the fast step of the inclusion reactions of **1**(HA⁻(○)), **1**(A²⁻(△)), and **2**(A²⁻(▲)) with DM- α CDx.

1(HA⁻) would easily take place. On the other hand, the inclusion of **2**(HA⁻ and A²⁻) and **3**(HA⁻ and A²⁻) would be fully blocked by a bulky alkyl group such as *i*Pr or *t*Bu. Ionization of the hydroxyl group of **1** also reduces the rate for inclusion or changes the direction for inclusion. Thus, the slow step is again observed in **1**(A²⁻).

The rate data presented in Table 3 demonstrate that the relative rate for inclusion which is possibly composed of a three-step mechanism is not appreciably affected by the sub-

SCHEME 5



stituent and/or the ionization of the hydroxyl group of the guest except for the **1**(HA⁻)-DM- α CDx system. These results suggest that the monitored dynamic inclusion process would be the analogous intramolecular step such as structural reorganization of the intermediate species. The lesser dependence of the rate constants on the steric factor and/or the ionization state of the guests as shown in Table 3 and Figures 4 and 7 supports this conclusion.

Finally, it is noteworthy that the effect of the di-*O*-methyl groups at the O(2) and O(6) positions of α CDx on the reactivity of inclusion is very large and brings about a drastic change of the reaction mechanism from two step to three step. The binding effects which have been observed in DM- α CDx system can be explained by the extended hydrophobicity of the cavity and/or around the rim of DM- α CDx, which must strengthen the binding ability with the guest. The existence of very rapid association equilibria (K_1 process) mainly results from the inclusion at the wider O(2)Me and O(3)H side of DM- α CDx than the secondary hydroxyl side of α CDx (Scheme 5). The enhanced inclusion stability of DM- α CDx with **1**, **2**, and **3** may be structurally explained by a more complete encapsulation of guest due to the enlarged hydrophobic cavity of the host (Scheme 5) and kinetically explained due to the smaller steric hindrance at the secondary hydroxyl (O(3)H and O(2)Me) side of DM- α CDx and to the existence of a multistep binding in the inclusion process.

References and Notes

- (1) (a) Cramer, F.; Saenger, W.; Spatz, H.-Ch. *J. Am. Chem. Soc.* **1967**, *89*, 14. (b) Yoshida, N.; Fujimoto, M. *Chem. Lett.* **1980**, 231 and 1377. (c) Yoshida, N.; Fujimoto, M. *Bull. Chem. Soc. Jpn.* **1982**, *55*, 1039. (d) Hersy, A.; Robinson, B. H. *J. Chem. Soc., Faraday Trans. 1* **1984**, *80*, 2039. (e) Schiller, R. L.; Coates, J. H.; Lincoln, S. F. *J. Chem. Soc., Faraday Trans. 1* **1984**, *80*, 1257. (f) Örstán, A.; Wojcik, F. *Carbohydr. Res.* **1985**, *143*, 43.
- (2) (a) Yoshida, N.; Fujimoto, M. *Chem. Lett.* **1984**, 703. (b) Yoshida, N.; Fujimoto, M. *J. Phys. Chem.* **1987**, *91*, 6691. (c) Yoshida, N.; Seiyama,

A.; Fujimoto, M. *J. Phys. Chem.* **1990**, *94*, 4246. (d) Yoshida, N.; Seiyama, A.; Fujimoto, M. *J. Phys. Chem.* **1990**, *94*, 4254. (e) Yoshida, N.; Hayashi, K. *J. Chem. Soc., Perkin Trans. 2* **1994**, 1285.

(3) Turro, N. J.; Okubo, T.; Chung, C.-J. *J. Am. Chem. Soc.* **1982**, *104*, 1789. Tran, C. D.; Fendler, J. H. *J. Phys. Chem.* **1984**, *88*, 2167. Hashimoto, S.; Thomas, J. K. *J. Am. Chem. Soc.* **1985**, *107*, 4655. Barra, M.; Bohne, C.; Scaiano, J. C. *J. Am. Chem. Soc.* **1990**, *112*, 8075. Bright, F. V.; Catena, G. C.; Huang, H. *J. Am. Chem. Soc.* **1990**, *112*, 1343. Mosseri, S.; Mialocq, J. C.; Perly, B. *J. Phys. Chem.* **1991**, *95*, 2196.

(4) Hybl, A.; Rundle, R. E.; Williams, D. E. *J. Am. Chem. Soc.* **1965**, *87*, 2779. Manor, P. C.; Saenger, W. *J. Am. Chem. Soc.* **1974**, *96*, 3630. Saenger, W.; Noltemeyer, M.; Manor, M.; Hingerty, P. C.; Klar, B. *Bioorg. Chem.* **1976**, *5*, 187. Harata, K. *Bull. Chem. Soc. Jpn.* **1976**, *49*, 2066. Wood, D. J.; Hruska, F. E.; Saenger, W. *J. Am. Chem. Soc.* **1977**, *99*, 1735.

(5) Bergeron, R.; Channig, M. A.; Gilbeily, G. J.; Pillor, D. M. *J. Am. Chem. Soc.* **1977**, *99*, 5146.

(6) Cramer, F. *Rev. Pure Appl. Chem.* **1955**, *5*, 143. Cramer, F. *Recl. Trav. Chim. Pays-Bas* **1956**, *75*, 891. Cramer, F.; Dietsche, W. *Chem. Ber.* **1959**, *5*, 1534. van Hooijdonk, C.; Breebaant-Hansen, J. C. A. E. *Recl. Trav. Chim. Pays-Bas* **1971**, *90*, 680. Jacobsen, J. *Int. J. Pept. Protein Res.* **1977**, *9*, 235. Laufer, R. B.; Vincent, A. C.; Padmanabhan, S.; Meade, T. J. *J. Am. Chem. Soc.* **1987**, *109*, 2216. Eliseev, A. V.; Schneider, H.-J. *J. Am. Chem. Soc.* **1994**, *116*, 6081. The hydrogen bond has been exploited to great effect in the design of a hydrogen-containing host which mainly acts in aprotic organic solvents and/or the solid state. See: Garciatellado, F.; Geib, S. J.; Goswami, S.; Hamilton, A. D. *J. Am. Chem. Soc.* **1991**, *113*, 9265. Adrian, J. C.; Wilcox, C. S. *J. Am. Chem. Soc.* **1992**, *114*, 1398. Kobayashi, K.; Ikeuchi, F.; Inaba, S.; Aoyama, Y. *J. Am. Chem. Soc.* **1992**, *114*, 1105. Sakaino, Y.; Takizawa, T.; Inouye, Y.; Kakisawa, H. *J. Chem. Soc., Perkin Trans. 2* **1986**, 1623. Sakaino, Y.; Fujii, R.; Fujiwara, T. *J. Chem. Soc., Perkin Trans. 1* **1990**, 2853.

(7) Casu, B.; Beggiani, M.; Sanderson, G. *Carbohydr. Res.* **1979**, *76*, 59. Gelb, R. I.; Schwartz, L. M.; Markinac, J. E.; Laufer, D. A. *J. Am. Chem. Soc.* **1979**, *101*, 1864. Harata, K.; Uekama, K.; Otagiri, M.; Hirayama, F. *Bull. Chem. Soc. Jpn.* **1982**, *55*, 407. Uekama, K. *Denpun Kagaku* **1983**, *30*, 247. Uekama, K.; Hirayama, F.; Imai, T.; Otagiri, M.; Harata, K. *Chem. Pharm. Bull.* **1983**, *31*, 3363. Szejtli, J. *J. Inclusion Phenom.* **1983**, *1*, 135. Yamamoto, Y.; Onda, M.; Takahashi, Y.; Inoue, Y.; Chujo, R. *Carbohydr. Res.* **1988**, *182*, 41. Green, A. R.; Guillory, J. K. *J. Pharm. Sci.* **1989**, *78*, 427. Kobayashi, N.; Osa, T. *Carbohydr. Res.* **1989**, *192*, 147. Kano, K.; Yoshiyasu, K.; Yasuoka, H.; Hata, S.; Hashimoto, S. *J. Chem. Soc., Perkin Trans. 2* **1992**, 1265. Harata, K.; Hirayama, F.; Arima, H.; Uekama, K.; Miyaji, T. *J. Chem. Soc., Perkin Trans. 2* **1992**, 1159.

(8) Harata, K.; Uekama, K.; Otagiri, M.; Hirayama, F. *Bull. Chem. Soc. Jpn.* **1982**, *55*, 3904.

(9) Szejtli, J. *Staerke* **1980**, *32*, 165.

(10) Szejtli, J. *Cyclodextrins and Their Inclusion Complexes*; Akademia Kiado: Budapest, Hungary, 1982; p 25.

(11) Harata, K. In *Inclusion Compounds*; Atwood, J. L., Davies, J. E. D., MacNicol, D. D., Eds.; Oxford University Press: New York, 1991, Vol. 5.

(12) Emert, J.; Breslow, R. *J. Am. Chem. Soc.* **1975**, *97*, 670. Tabushi, I.; Shimokawa, K.; Shimizu, N.; Shirakata, H.; Fujita, K. *J. Am. Chem. Soc.* **1976**, *98*, 7855.

(13) Nakai, Y.; Yamamoto, K.; Terada, K.; Oguchi, T.; Nakamura, G. *Yakugaku Zasshi* **1987**, *107*, 802. Brettinetti, G.; Melani, F.; Mura, P.; Monnanni, R.; Giordano, F. *J. Pharm. Sci.* **1991**, *80*, 1162.

(14) Harada, A.; Takahashi, S. *J. Chem. Soc., Chem. Commun.* **1987**, 527.

(15) Bertrand, G. L.; Faulkner, J. R.; Han, S. M.; Armstrong, D. W. *J. Phys. Chem.* **1989**, *93*, 6863.

JP9426841